

INCREASING NUMERICAL EFFICIENCY IN COUPLED EULERIAN-LAGRANGIAN METAL FORMING SIMULATIONS

FRANZ HAMMELMÜLLER AND CHRISTIAN ZEHETNER

Linz Center of Mechatronics (LCM)
Altenbergerstrasse 69, 4040 Linz, Austria
e-mail: franz.hammelmuller@lcm.at, www.lcm.at

Key words: Computational Plasticity, Metal Forming, Coupled Euler-Lagrange.

Abstract. The coupled Eulerian-Lagrangian formulation is an efficient tool for modelling and simulation of metal forming processes with large deformation. In many cases, thermo-mechanical coupling has to be considered. Usually the numerical effort is very high for such processes, and large simulation times are the consequence. In this paper, strategies for reducing the simulation time are investigated, based on the example of a hot forming process.

1 INTRODUCTION

The coupled Eulerian-Lagrangian formulation is an efficient tool to model and simulate metal forming processes with large plastic deformations. In order to control and optimize such processes with respect to cycle time, life time of the tools and quality of the product, detailed numerical simulation models are necessary. Usually, the numerical effort is very high for such kinds of problems.

In this paper, two strategies for reducing the simulation time are investigated for the example of a hot cylinder pressed into a die by a moving stamp. For this process a three-dimensional Finite Element model is implemented using the software package ABAQUS, version 6.12-1. The tools (stamp and die) are represented by Lagrangian three-dimensional Finite Elements, and the work piece by three-dimensional Eulerian Finite Elements. Contact is implemented between tools and work-piece and an explicit dynamic coupled thermo-mechanical simulation is performed.

Implementing the simulation model with all the relevant physical parameters yields a very long computation time. In commercial software tools as ABAQUS, strategies like mass scaling are implemented in order to reduce simulation times. However, ABAQUS does not provide the mass scaling feature for Eulerian Elements. Two strategies are investigated in this paper to overcome this restriction and to reduce simulation time. First, mass scaling is realized by scaling the parameters for density. Secondly, time scaling is implemented by transforming the time scale to a fictitious one. However, in both cases also the thermal properties have been adapted in order to maintain the thermal time constant.

Based on the implemented metal forming process, these approaches are compared, and it is shown that by an appropriate scaling of the physical parameters, the simulation time can be reduced by several orders of magnitude without loss of accuracy of the results.

2 THERMO-MECHANICAL COUPLED FORMING PROCESS

In the following, a forming process according to Figure 1 is considered. A hot work piece is pressed into a die by a moving stamp. Die and stamp are considered to be linear elastic, and for the work piece an exponential flow curve is assumed depending on temperature. Initially the temperature of the tools is room temperature, and the work piece is heated to 1080°C.

The model has been implemented in ABAQUS as follows: The tools are represented by Lagrangian Finite Elements, and the work piece by Eulerian Finite Elements. Mechanical and thermal contact is defined between the parts.

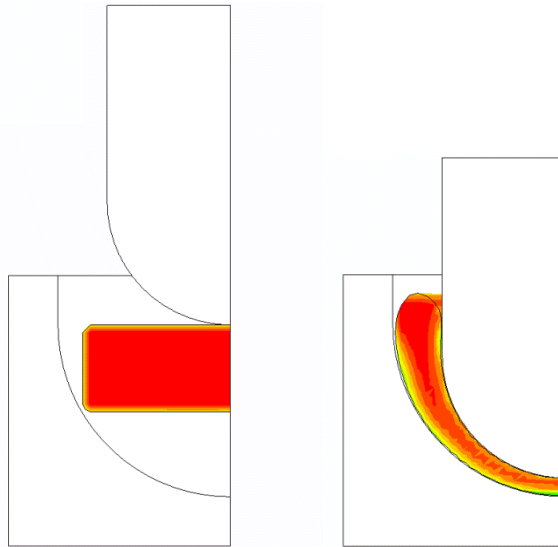


Figure 1: Forming Process

The motion of the stamp is slow, such that inertial forces can be neglected. From this point of view the mechanical behavior is quasi-static. Moreover the strain rates are small. On the other hand side, transient thermal behavior has to be considered. Using ABAQUS, an explicit dynamic coupled thermo-mechanical analysis has been defined.

It has turned out that even for such a simple forming process very large computation times are obtained. Due to the negligible inertial forces, the explicit solver requires very small time increments in order to achieve a stable solution.

A reduction of the computation time is possible by either scaling time or mass, assuming that strain rates and inertial forces remain small. For retaining the correct thermal time constants, the thermal parameters have to be adapted appropriately. The principal approach is demonstrated in section 3 for the linear thermo-elastic case. The numerical results for the nonlinear forming process according to Figure 1 are summarized in section 4.

3 COUPLED LINEAR THERMOELASTICITY

The following formulations are referred to Nicholson [3]. The constitutive equation for linear thermo-elastic behavior are given as

$$\mathbf{T} = 2\mu\mathbf{E} + \lambda[\text{tr}(\mathbf{E}) - \alpha(T - T_0)]\mathbf{I}, \quad (1)$$

where \mathbf{T} is the stress tensor, \mathbf{E} the linear strain tensor, λ and μ are Lamé coefficients, T is the actual temperature, T_0 the reference temperature, α is the thermal expansion coefficient and \mathbf{I} the identity matrix. The strain tensor is related to the displacement vector \mathbf{u} as

$$\mathbf{E} = \frac{1}{2}(\nabla\mathbf{u} + \nabla\mathbf{u}^T), \quad (2)$$

The thermal field equation is written as

$$-k\nabla^2 T = \alpha\lambda T_0 \text{tr}(\dot{\mathbf{E}}) + \rho c_e \dot{T}, \quad (3)$$

with the conductivity k , density ρ and specific heat c_e . The first term on the right hand side considers the influence of strain rate on the temperature field. In the static case this coupling term vanishes. The mechanical behavior is formulated by Navier's equations for thermoelasticity,

$$\mu\nabla^2\mathbf{u} + (\lambda + \mu)\nabla\text{tr}(\mathbf{E}) - \alpha\lambda\nabla T = \rho\frac{\partial\mathbf{u}}{\partial t^2}. \quad (4)$$

The influence of temperature on the mechanical field, i.e. the thermal expansion is considered by the third term on the left hand side.

4 STRATEGIES FOR MINIMIZING THE COMPUTATION TIME

In the following, two strategies for minimizing the computation time are investigated: Mass scaling and time scaling. In both cases, the thermal properties have to be adapted in order to retain the thermal time constant. Mass scaling can be applied even when there is rate dependency, or when the parameters are time-dependent. Scaling time is only possible when the parameters do not depend on time, and when rate dependency is negligible.

4.1 Mass scaling

The mass in Eq. (4) is scaled by replacing density ρ by the fictitious density $\rho^* = \kappa_m\rho$, $\kappa_m > 1$. The magnitude of κ_m has to be chosen such that the inertial forces represented by the right hand side in Eq. (4) remain small. When substituting the density ρ by a fictitious density ρ^* , the thermal time constant in Eq. (3) changes. This effect can be compensated by introducing the fictitious specific heat $c_e^* = c_e\kappa_m^{-1}$. From Eqs. (3) and (4) follow the scaled thermo-elastic equations:

$$-k\nabla^2 T = \alpha\lambda T_0 \text{tr}(\dot{\mathbf{E}}) + \rho^* c_e^* \dot{T}, \quad (5)$$

$$\mu\nabla^2 \mathbf{u} + (\lambda + \mu)\nabla \text{tr}(\mathbf{E}) - \alpha\lambda \nabla T = \rho^* \frac{\partial \mathbf{u}}{\partial t^2}. \quad (6)$$

Since the right hand side of Eq. (6) has increased, the minimal stable time increment of the explicit solver is enlarged.

4.2 Time scaling

Replacing time t in Eq. (4) by the fictitious time $\tau = t\kappa_t^{-1}$, $\kappa_t > 1$, has the same consequence on the inertial force as mass scaling in section 4.1, with the relation $\kappa_t^2 = \kappa_m$. Again, the thermal parameters have to be adapted, e.g. by introducing the fictitious specific heat $c_e^* = c_e \kappa_t^{-1}$. Note that this strategy is only allowed for the case that the influence of the strain rate $\dot{\mathbf{E}}$ is negligible.

$$-k\nabla^2 T = \alpha\lambda T_0 \text{tr}\left(\kappa_t \frac{d\mathbf{E}}{d\tau}\right) + \rho c_e^* \frac{dT}{d\tau}, \quad (7)$$

$$\mu\nabla^2 \mathbf{u} + (\lambda + \mu)\nabla \text{tr}(\mathbf{E}) - \alpha\lambda \nabla T = \rho \frac{\partial \mathbf{u}}{\partial \tau^2}. \quad (8)$$

5 NUMERICAL STUDY

In section 4, two speed-up strategies have been stated for the linear case. In this section, these strategies are applied to the nonlinear forming process shown in section 2.

5.1. Simulation model

The Finite Element simulation model has been implemented in ABAQUS. The tools, i.e the stamp and die are represented by the Lagrangian Finite Elements of type C3D8T, the hot work piece by Eulerian Elements of type EC3D8RT. These elements consider thermomechanical coupling. For the tools linear elastic behavior, and for the work piece elasto-plastic behavior has been implemented. Young's modulus and the flow curve depend on temperature. As thermal properties, the specific heat and thermal conduction have been defined for both materials. The material parameters are shown in Tables 1 and 2.

Furthermore, contact has been defined between the tools and the work piece. The interaction of Lagrangian and Eulerian Finite Elements is realized by a Penalty-based contact formulation. For the thermal contact, a pressure dependent gap conductance has been defined.

Table 1: Parameters for the tools (stamp and die)

Stamp	radius	m	0.10	
	height	m	0.26	
Die	radius	m	0.18	
	height	m	0.26	
Material	density	kg/m ³	7850	
	thermal conductivity	W/(mK)	30	
	specific heat	J/K	452	
	Young's modulus	N/m ²	temperature 0°C	temperature 1000°C
			2.1e11	1.05e11

Table 2: Parameters for the work piece

Hot cylinder	radius	m	0.12	
	height	m	0.071	
Material	density	kg/m ³	7850	
	thermal conductivity	W/(mK)	30	
	specific heat	J/K	452	
	Young's modulus	N/m ²	temperature 0°C	temperature 1000°C
	yield stress	N/m ²	2.1e11	1.05e11
			2.17e8	9.2e7

The solutions are obtained by an explicit thermo-mechanical coupled transient analysis. Both, time and mass scaling strategies have been implemented by defining fictitious parameters for mass/time and specific heat. Parameter studies have been performed with respect to the scaling parameters κ_m and κ_t . The results are shown in the following section.

5.2. Numerical results

A main indicator for the appropriateness of the solution is the smoothness of the contact force. Figure 2 shows the contact force as a parameter of the time and mass scale factor, respectively. Note that the two scaling strategies yield almost equal results for $\kappa_t = \sqrt{\kappa_m}$. A smooth contact force, as expected for the quasi-static case, is obtained for $\kappa_t \leq 20$. For the case $\kappa_t = 100$ the kinetic energy is dominating at the beginning of the process. Due to the impact between tool and work piece oscillations with high amplitude are caused. Immediately after the impact, the assumption of a quasi-static process is no more valid. However, after the decay of the oscillations a smooth contact force is obtained. For this state, also with the high time scale parameter a good estimation of the contact force is obtained.

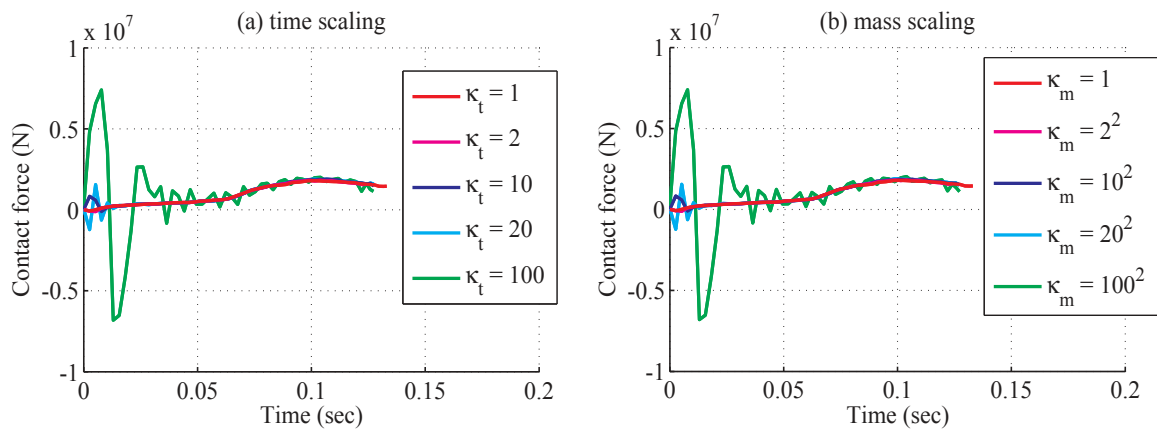


Figure 2: Contact force (a) time scaling (b) mass scaling

Secondly, the displacement and temperature fields are compared in Figure 3. Both scaling strategies yield an equal result. Compared to the unscaled case, the results show negligible differences.

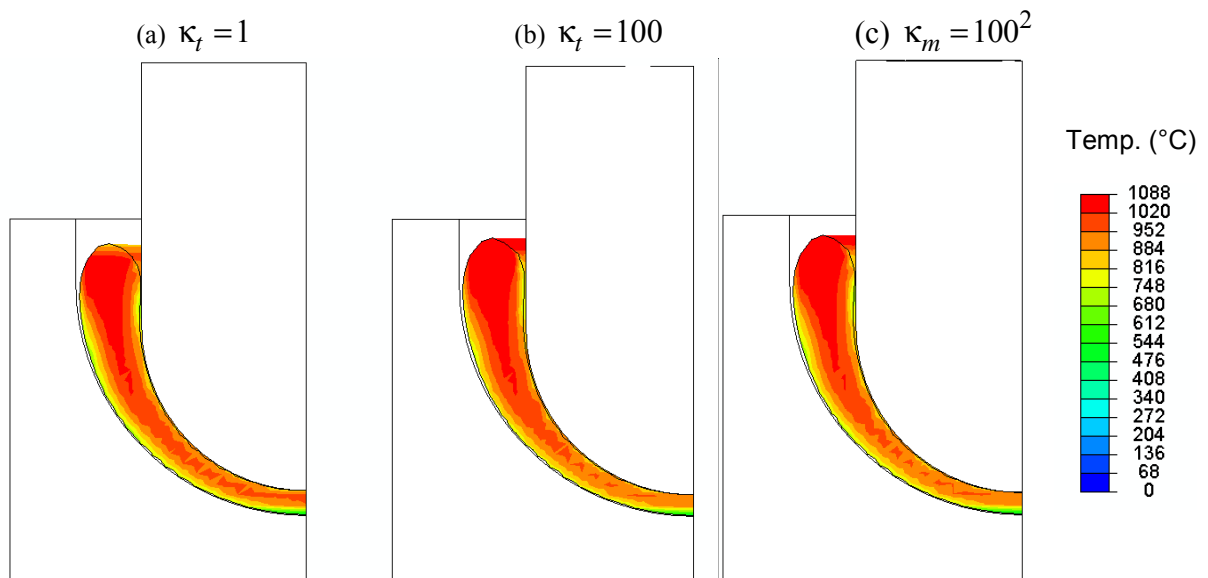


Figure 3: Displacement and temperature fields (a) $\kappa_t = \kappa_m = 1$ (b) time scaling $\kappa_t = 100$, (c) mass scaling $\kappa_m = 100^2$

Finally, the computation time has been analyzed. Figure 4a shows the influence of the time scaling factors on the cpu-time. Note that for $\kappa_t = \sqrt{\kappa_m}$ the same numerical efficiency has been expected. A significant decrease of the simulation time is obtained comparing the scale factors $\kappa_t = 1$ and $\kappa_t = 20$. A further enlargement of the scaling factor only slightly reduces the computation time. In Figure 2 the comparison of $\kappa_t = 1$ and $\kappa_t = 20$ has shown a very good coincidence of the resulting contact force. Thus, with respect to simulation time and accuracy of the solution a factor of $\kappa_t = 20$ seems to be a good choice in this case.

In Figure 4b the speed-up factor is shown as a function of the scaling factor, showing a linear dependency. This has to be expected in an explicit dynamic analysis for time scaling. Reducing the time period and solving with the same time increment yields a speed-up of the simulation time with the same factor.

Note that numerical efficiency of time scaling seems to be higher. The computations have been performed on the same computer. Maybe the processor load may have been different for the two parameter studies. On the other hand, the thermo-elastic equations do differ for the two scaling strategies. Further investigations are necessary to clarify this behavior. However, speed-up factors with the same order of magnitude are obtained with both strategies. Mass scaling may be advantageous in case of time-dependent parameters or rate-dependent problems.

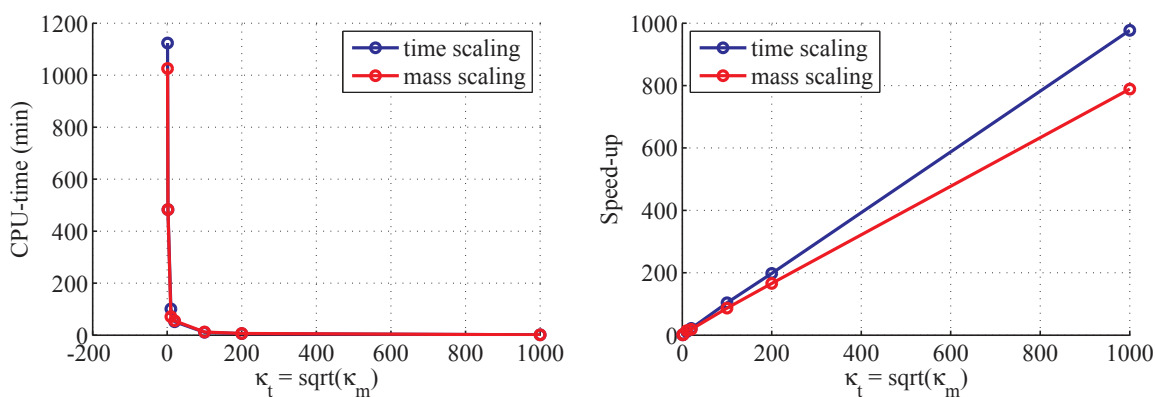


Figure 4: (a) CPU-time in minutes, (b) Speed-up factor

6 CONCLUSIONS

It has been shown how the numerical efficiency can be increased in the simulation of metal forming processes. For the example of a hot pressing process two strategies have been investigated, i.e. time scaling and mass scaling. It has been shown that computation time can be reduced significantly without loss of accuracy of the result. For the considered example, optimal scaling factors have been determined with respect to simulation time and accuracy. The obtained knowledge is especially valuable for the simulation of complex industrial applications.

REFERENCES

- [1] Benson, D.J. Computational Methods in Lagrangian and Eulerian Hydrocodes, *Comp. Meth. Appl. Mech. Engng* (1992) **99**, 235–394.
- [2] Stanier, L., Yang, Q. and Ortiz, M., On the variational formulation of nonlinear coupled thermomechanical constitutive equations and updates, *Proceedings of VIII International Conference on Computational Plasticity (COMPLAS VIII)*, E. Onate and D.R.J. Owen (Eds), Barcelona (2005).
- [3] Nicholson, D.W. *Finite element analysis: thermomechanics of solids*, CRC Press (2008)